

## **Viscosities of Multicomponent Silicate Melts at High Temperatures<sup>1</sup>**

**F.-Z. Ji,<sup>2</sup> D. Sichen,<sup>2,3</sup> and S. Seetharaman<sup>2</sup>**

---

In the present work; the viscosities in the quaternaries CaO-Fe<sub>n</sub>O-MgO-SiO<sub>2</sub>, Fe<sub>n</sub>O-MgO-MnO-SiO<sub>2</sub>, and CaO-MgO-MnO-SiO<sub>2</sub> and the quinary CaO-Fe<sub>n</sub>O-MgO-MnO-SiO<sub>2</sub> were studied. The experimental technique employed was the well-established rotating cylinder method, using a Brookfield digital viscometer mounted over a specially designed graphite furnace. Generally, iron crucibles were used along with iron spindles. Periodic calibrations of the experimental setup were made using the standard reference slag recommended by the European Union. The measurements were carried out up to a maximum temperature of 1773 K in all cases. The reliability of the measurements were checked at different rotation speeds as well as during thermal cycling, and excellent reproducibility of the results was noted. The experimental viscosity values were incorporated into a viscosity model. Equations based on the model for calculating the viscosities of the quaternary systems CaO-Fe<sub>n</sub>O-MgO-SiO<sub>2</sub>, Fe<sub>n</sub>O-MgO-MnO-SiO<sub>2</sub>, and CaO-MgO-MnO-SiO<sub>2</sub> and the quinary system CaO-Fe<sub>n</sub>O-MgO-MnO-SiO<sub>2</sub> are provided.

---

**KEY WORDS:** experiment; model; silicate melts; viscosity.

### **1. INTRODUCTION**

The viscosities of silicate melts are of great importance in metallurgical and glass industries. An attempt is currently being made in the present laboratory to get a complete description of viscosities in the multicomponent system, Al<sub>2</sub>O<sub>3</sub>-CaO-Cr<sub>2</sub>O<sub>3</sub>-FeO-Fe<sub>2</sub>O<sub>3</sub>-MgO-MnO-SiO<sub>2</sub>. In order to achieve this task, a mathematical model for estimating the

---

<sup>1</sup> Paper presented at the Thirteenth Symposium on Thermophysical Properties, June 22-27, 1997, Boulder, Colorado, U.S.A.

<sup>2</sup> Division of Theoretical Metallurgy, Royal Institute of Technology, S-10044 Stockholm, Sweden.

<sup>3</sup> To whom correspondence should be addressed.

viscosities of multicomponent slags has been developed [1]. The model has recently been slightly modified [2]. It is found that the modified version is not only able to express viscosity as a function of temperature and composition, but it also successful in predicting viscosities of higher-order ionic melts using information for the corresponding lower-order systems. A reliable description of the multicomponent system using this model assumes that accurate experimental data for the corresponding lower-order systems are available. A series of experimental measurements of the viscosities of the binary and ternary silicate melts [3, 4] have been carried out previously. Following this, the objective of the present work is to study the viscosities of the quaternaries  $\text{CaO-Fe}_n\text{O-MgO-SiO}_2$ ,  $\text{Fe}_n\text{O-MgO-MnO-SiO}_2$ , and  $\text{CaO-MgO-MnO-SiO}_2$  and the quinary  $\text{CaO-Fe}_n\text{O-MgO-MnO-SiO}_2$ . No experimental viscosity data for these systems could be found in the literature except for the  $\text{CaO-MgO-MnO-SiO}_2$  system. Tanabe [5] has observed the iso-viscosity contours for the system  $\text{CaO-MgO-MnO-SiO}_2$  at 1713 K and 16 mass% MnO. However, these isolines are associated with very high uncertainties, as high as 100%. While the experimental data obtained in the present work will enhance our viscosity databank, they will also provide a measure of the reliability of the viscosity model.

## 2. EXPERIMENTAL

### 2.1. Materials and Preparation of the Slags

The materials used in the present work along with their purities and suppliers are presented in Table I. While the  $\text{MnO}$  powder and  $\text{Fe}_2\text{O}_3$  powder were dried at 393 K overnight, the  $\text{CaO}$ ,  $\text{MgO}$  and  $\text{SiO}_2$  powders were calcined at 1223 K for 12 h in a muffle furnace to decompose any carbonate or hydroxide before use. The procedure of the preparation of the

Table I. Materials Used in the Present Study

Material	Purity	Supplied by
Calcium oxide ( $\text{CaO}$ )	Anhydrous, AR grade	Fisher Scientific, NJ, U.S.A.
Iron ( $\text{Fe}$ )	Pro analyze grade	E. Merck, Darmstadt, Germany
Iron oxide ( $\text{Fe}_2\text{O}_3$ )	Anhydrous, AR grade	Fisher Scientific, NJ, U.S.A.
Magnesium oxide ( $\text{MgO}$ )	Pro analyze grade	E. Merck, Darmstadt, Germany
Manganese oxide ( $\text{MnO}$ )	99.5% purity	Johnson Matthey, GmbH, Germany
Silicon oxide ( $\text{SiO}_2$ )	Pro analyze grade	E. Merck, Darmstadt, Germany
Argon ( $\text{Ar}$ )	Argon plus ( $\text{Ar} > 99.99\%$ )	AGA Gas, Stockholm, Sweden

**Table II.** Dimensions of Crucibles and Spindles Used in the Present Work

Crucible (mm)			Spindle (mm)	
Pure iron (Armco iron)	I.D.	40	Bob diam.	16
	Wall thickness	3	Length of bob	27
	Inner depth	95	Shaft diam.	4
	Base thickness	8	Length of shaft	54
	Total height	103	Angle for the tapers	45°

slags has been described in detail in a previous publication [3]. In order to get the accurate  $Fe_nO$  content in the slag, iron and  $Fe_2O_3$  powders of required proportions were first mixed. The Fe- $Fe_2O_3$  mixture had a total composition of 51 mol% oxygen, at which liquid oxide would be in equilibrium with  $\delta$ -Fe at temperatures around 1673 K [6]. The Fe- $Fe_2O_3$  mixture was then mixed well with other powders for premelting. Crucibles made of pure iron (Armco iron) were used for the premelting of the slags. The dimensions of the iron crucibles are listed in Table II. The slag was melted in a resistance furnace under a purified argon atmosphere. The oxygen partial pressure of the gas was monitored constantly by a  $ZrO_2$ -CaO oxygen probe and found to be about  $10^{-9}$  bar during both the preparation of the slags and the viscosity measurements. After premelting, the slag was ocularly examined to ascertain that the sample had been completely molten. The slag along with the crucible was then stored in a desiccator prior to the viscosity measurements.

## 2.2. Apparatus and Procedure

The viscosity measurements were carried out with a Brookfield digital viscometer (Model RVDV-III; full-scale torque,  $7.187 \times 10^{-4}$  N·m) using the rotating cylinder method. The experimental setup and procedure have been described in detail in an earlier publication [3]. Figure 1 shows the viscometer mounted on top of a high-temperature furnace (Laboratory Furnace Group 1000 supplied by Thermal Technology Inc.). The iron crucible used for the premelting of the slag was later employed for the viscosity measurement. Pure iron spindles were used in the experiments. The dimensions of the iron spindles are presented in Table II.

In a general run, the spindle mounted on the transducer was introduced into the alumina reaction tube and located 1 cm above the slag that was placed in the even-temperature zone of the furnace. Teflon bellows connected to the viscometer and metal flange on the top of the alumina tube were used to seal the reaction chamber. The slag was heated up to the

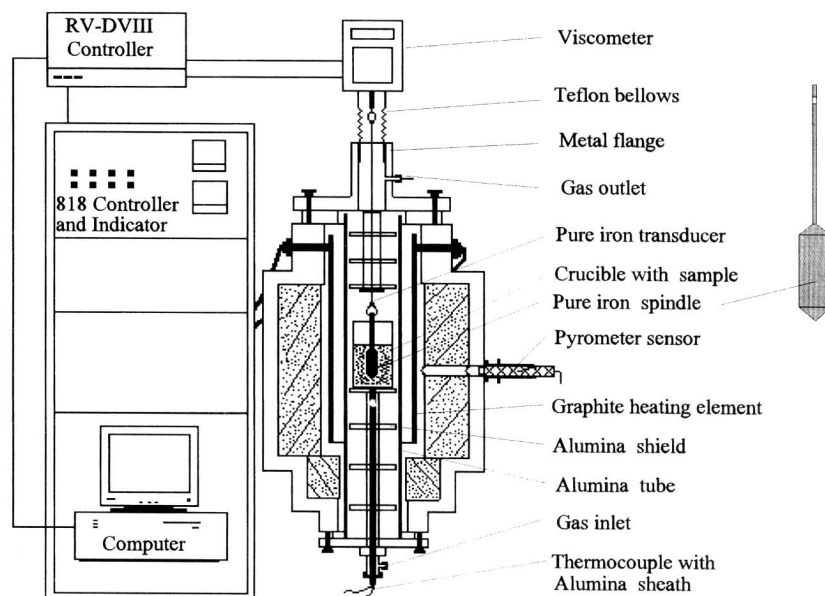


Fig. 1. Experimental setup.

desired temperature at a heating rate of  $5 \text{ K} \cdot \text{min}^{-1}$  under a purified argon atmosphere. When the temperature was stabilized, the spindle, rotating at a speed of 40–60 rpm, was introduced into the molten slag by adjusting the length of the Teflon bellows. The tip of the spindle was located 1.2 cm above the crucible base, and the length of the shaft immersed in the melt was 1.0 cm. The thermal equilibration time at each temperature set point was chosen to be 30 min. Viscosity measurements were carried out using five rotation rates. The equilibration time for viscosity measurement at each speed of rotation was 2 min.

The viscometer was calibrated using four mineral oil standards with viscosities of 0.0985, 0.960, 4.850, and  $12.500 \text{ Pa} \cdot \text{s}$  at  $298.0 \pm 0.1 \text{ K}$ . Calibrations of the viscometer were also made in the temperature range of 1463 to 1675 K using a reference slag (consisting of  $\text{Li}_2\text{O}-\text{Al}_2\text{O}_3-\text{SiO}_2$ ), developed for the BCR program of the European Union [7].

After the viscosity measurements, some of the slags were randomly chosen for chemical analysis. For this purpose, a sequential X-ray spectrometer SRS303 supplied by Siemens was employed. The contents of the oxides obtained by analysis were in agreement with the weighed-in amounts within  $\pm 1\%$ .

### 3. RESULTS

A number of slags in each system were studied. Tables III to VI present the experimental results for the systems, CaO-Fe<sub>n</sub>O-MgO-SiO<sub>2</sub>, Fe<sub>n</sub>O-MgO-MnO-SiO<sub>2</sub>, CaO-MgO-MnO-SiO<sub>2</sub>, and CaO-Fe<sub>n</sub>O-MgO-MnO-SiO<sub>2</sub>, respectively. As mentioned above, viscosity measurements

**Table III.** Measured Viscosities in the CaO-Fe<sub>n</sub>O-MgO-SiO<sub>2</sub> System

Temperature (K)	CaO (mass %)	Fe <sub>n</sub> O (mass %)	MgO (mass %)	Viscosity (dPa · s)
1773	21.6	10.0	9.0	10.00
1723	21.6	10.0	9.0	13.26
1673	21.6	10.0	9.0	20.94
1653	21.6	10.0	9.0	31.45
1773	22.5	10.0	22.5	2.60
1753	22.5	10.0	22.5	2.98
1733	22.5	10.0	22.5	3.38
1723	22.5	10.0	22.5	3.61
1703	22.5	10.0	22.5	4.05
1783	22.5	10.0	22.5	4.61
1673	22.5	10.0	22.5	4.84
1653	22.5	10.0	22.5	5.59
1633	22.5	10.0	22.5	6.48
1623	22.5	10.0	22.5	7.03
1603	22.5	10.0	22.5	8.22
1583	22.5	10.0	22.5	9.96
1573	22.5	10.0	22.5	10.74
1561	22.5	10.0	22.5	12.34
1543	22.5	10.0	22.5	14.43
1773	7.00	30.0	17.5	1.30
1763	7.00	30.0	17.5	1.37
1753	7.00	30.0	17.5	1.46
1738	7.00	30.0	17.5	1.56
1723	7.00	30.0	17.5	1.68
1713	7.00	30.0	17.5	1.75
1708	7.00	30.0	17.5	1.87
1698	7.00	30.0	17.5	2.19
1688	7.00	30.0	17.5	2.24
1673	7.00	30.0	17.5	3.44
1773	18.75	25.0	18.75	1.07
1763	18.75	25.0	18.75	1.11
1753	18.75	25.0	18.75	1.13
1740	18.75	25.0	18.75	1.23
1723	18.75	25.0	18.75	1.44
1711	18.75	25.0	18.75	2.04
1695	18.75	25.0	18.75	2.51

Table IV. Measured Viscosities in the CaO–MgO–MnO–SiO<sub>2</sub> System

Temperature (K)	CaO (mass %)	MgO (mass %)	MnO (mass %)	Viscosity (dPa · s)
1773	21.6	9.0	10.0	9.29
1753	21.6	9.0	10.0	10.72
1733	21.6	9.0	10.0	12.42
1723	21.6	9.0	10.0	13.40
1712	21.6	9.0	10.0	14.78
1693	21.6	9.0	10.0	17.48
1673	21.6	9.0	10.0	20.96
1653	21.6	9.0	10.0	23.04
1648	21.6	9.0	10.0	26.13
1633	21.6	9.0	10.0	30.63
1623	21.6	9.0	10.0	33.76
1608	21.6	9.0	10.0	39.34
1593	21.6	9.0	10.0	46.62
1773	7.00	17.5	30.0	1.59
1743	7.00	17.5	30.0	1.84
1723	7.00	17.5	30.0	2.22
1708	7.00	17.5	30.0	2.84
1773	20.0	20.0	20.0	1.28
1753	20.0	20.0	20.0	1.74
1743	20.0	20.0	20.0	2.12
1733	20.0	20.0	20.0	2.69
1773	22.5	22.5	10.0	2.06
1763	22.5	22.5	10.0	2.30
1753	22.5	22.5	10.0	2.54
1743	22.5	22.5	10.0	2.99
1733	22.5	22.5	10.0	3.60
1723	22.5	22.5	10.0	4.54
1708	22.5	22.5	10.0	6.16

were carried out using five rotation rates at each temperature. The viscosity values listed in Tables III to VI are the average values for the experimental data obtained using five rotation rates. The maximum deviation of the experimental data from the mean values was generally found to be less than 1%.

As mentioned earlier, only viscosities of the CaO–MgO–MnO–SiO<sub>2</sub> system with 16 mass% MnO at 1713 K have been reported earlier [5]. It is difficult to compare these isoviscosity lines with the present results, in view of the high uncertainties in the former work.

Table V. Measured Viscosities in the  $\text{Fe}_n\text{O-MgO-MnO-SiO}_2$  System

Temperature (K)	$\text{Fe}_n\text{O}$ (mass%)	$\text{MgO}$ (mass%)	$\text{MnO}$ (mass%)	Viscosity (dPa · s)
1773	30.0	5.60	28.0	0.55
1733	30.0	5.60	28.0	0.58
1753	30.0	5.60	28.0	0.60
1743	30.0	5.60	28.0	0.61
1733	30.0	5.60	28.0	0.66
1723	30.0	5.60	28.0	0.71
1703	30.0	5.60	28.0	0.80
1683	30.0	5.60	28.0	0.87
1673	30.0	5.60	28.0	0.97
1653	30.0	5.60	28.0	1.02
1773	10.0	7.20	36.0	3.35
1763	10.0	7.20	36.0	3.45
1753	10.0	7.20	36.0	3.65
1743	10.0	7.20	36.0	4.21
1731	10.0	7.20	36.0	4.79
1723	10.0	7.20	36.0	5.04
1703	10.0	7.20	36.0	5.94
1683	10.0	7.20	36.0	7.45
1673	10.0	7.20	36.0	8.18
1653	10.0	7.20	36.0	9.72
1773	10.0	24.3	13.5	1.91
1763	10.0	24.3	13.5	1.99
1751	10.0	24.3	13.5	2.35
1743	10.0	24.3	13.5	2.86
1738	10.0	24.3	13.5	4.54
1731	10.0	24.3	13.5	4.96

#### 4. DISCUSSION

On the basis of the viscosity model [2], which is a modified version of an earlier model developed in the present laboratory [1], the viscosities of the quarternary and quinary silicate melts can be predicted using the available model parameters with up-to-ternary interactions. In this model, the Temkin description of the ionic solution is adopted, which classifies the cations and anions in different subgroupings. For example, a silicate solution,  $\text{CaO-Fe}_n\text{O-MgO-MnO-SiO}_2$  can be represented by

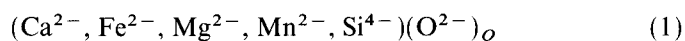


Table VI. Measured Viscosities in the CaO-Fe<sub>n</sub>O-MgO-MnO-SiO<sub>2</sub> System

Temperature (K)	CaO (mass %)	Fe <sub>n</sub> O (mass %)	MgO (mass %)	MnO (mass %)	Viscosity (dPa · s)
1773	17.5	18.0	17.5	12.0	0.58
1755	17.5	18.0	17.5	12.0	0.68
1741	17.5	18.0	17.5	12.0	0.98
1723	17.5	18.0	17.5	12.0	1.50
1713	17.5	18.0	17.5	12.0	1.89
1773	31.68	10.8	12.47	7.20	1.05
1761	31.68	10.8	12.47	7.20	1.09
1748	31.68	10.8	12.47	7.20	1.16
1733	31.68	10.8	12.47	7.20	1.25
1723	31.68	10.8	12.47	7.20	1.33
1709	31.68	10.8	12.47	7.20	1.47
1688	31.68	10.8	12.47	7.20	1.69
1773	7.0	18.0	16.1	12.0	1.87
1753	7.0	18.0	16.1	12.0	2.15
1733	7.0	18.0	16.1	12.0	2.37
1723	7.0	18.0	16.1	12.0	2.49
1701	7.0	18.0	16.1	12.0	3.16
1681	7.0	18.0	16.1	12.0	3.92
1673	7.0	18.0	16.1	12.0	4.09
1653	7.0	18.0	16.1	12.0	7.20
1773	16.1	18.0	7.0	12.0	1.98
1759	16.1	18.0	7.0	12.0	2.10
1743	16.1	18.0	7.0	12.0	2.28
1733	16.1	18.0	7.0	12.0	2.42
1723	16.1	18.0	7.0	12.0	2.55
1708	16.1	18.0	7.0	12.0	2.80
1688	16.1	18.0	7.0	12.0	3.18
1673	16.1	18.0	7.0	12.0	3.40
1653	16.1	18.0	7.0	12.0	3.98
1633	16.1	18.0	7.0	12.0	4.64
1623	16.1	18.0	7.0	12.0	5.00
1597	16.1	18.0	7.0	12.0	6.00
1573	16.1	18.0	7.0	12.0	7.19
1548	16.1	18.0	7.0	12.0	8.88
1523	16.1	18.0	7.0	12.0	11.27



where  $Q$  is the stoichiometric coefficient. The ionic fraction of cations Ci within the cation group is defined as

$$y_{\text{Ci}} = \frac{N_{\text{Ci}}}{\sum N_{\text{C}}} \quad (2)$$

where  $N_{\text{Ci}}$  represents the number of the Ci cations and the summation covers all the cations in the system. In the case of all the quarternary and quinary systems studied, the cation fractions happen to be the same as the mole fractions of the corresponding oxide components.

According to this model, the viscosity,  $\eta$ , can be expressed as

$$\eta = \frac{hN\rho}{M} \exp\left(\frac{\Delta G^*}{RT}\right) \quad (3)$$

where  $h$  is Plank's constant,  $N$  is Avogadro's number,  $R$  is the gas constant,  $T$  is the temperature in kelvin, and  $\rho$  and  $M$  are the density and molecular weight of the melt, respectively. The  $\Delta G^*$  in Eq. (3) is the Gibbs energy of activation for viscosity, which is a function of both temperature and composition of the melt. The molecular weight of a melt can be calculated by

$$M = \sum X_i M_i \quad (4)$$

where  $X_i$  and  $M_i$  represent the mole fraction and the molecular weight of component  $i$  in the solution, respectively. In the model, as a first approximation, the density of a multicomponent melt is expressed by the average density of the solution:

$$\rho = \sum X_i \rho_i \quad (5)$$

where  $\rho_i$  is the density of pure component  $i$  in the liquid state.

The Gibbs energy of activation for viscosity in Eq. (3) can be expressed as

$$\Delta G^* = \sum X_i \Delta G_i^* + \Delta G_{\text{Mix}}^* \quad (6)$$

$\Delta G_i^*$  is the Gibbs energy of activation of pure component  $i$  in the liquid state and is usually a linear function of temperature. The effect of the interactions between different species on  $\Delta G^*$  is attributed to the second term in Eq. (6). In the case of oxide systems, only the interactions of different cations in the presence of  $\text{O}^{2-}$  ions are taken into account. The term

$\Delta G_{\text{Mix}}^*$  is expressed as polynomials of cation fractions and temperature [1, 2].

The relevant model parameters with up-to-ternary interactions have been optimized using the experimental data for the corresponding unary, binary, and ternary systems [2]. These parameters are presented in Table VII along with the density data that are necessary for the model calculations. The viscosities of the CaO–Fe<sub>n</sub>O–MgO–SiO<sub>2</sub>, Fe<sub>n</sub>O–MgO–MnO–SiO<sub>2</sub>, CaO–MgO–MnO–SiO<sub>2</sub>, and CaO–Fe<sub>n</sub>O–MgO–MnO–SiO<sub>2</sub> melts could be calculated using the above viscosity model [2]. In view of the similarity of the cations, Ca<sup>2+</sup>, Fe<sup>2+</sup>, Mg<sup>2+</sup>, and Mn<sup>2+</sup>, the binary interactions between these ions were not considered in the model calculations. To help the readers to use the model, the expressions of the Gibbs activation energies for the viscosities in the four systems are given in Eqs. (7) to (10), respectively.

$$\begin{aligned} \Delta G^*(\text{CaO-Fe}_n\text{O-MgO-SiO}_2) &= [X_{\text{CaO}} \Delta G_{\text{CaO}}^* + X_{\text{Fe}_n\text{O}} \Delta G_{\text{Fe}_n\text{O}}^* + X_{\text{MgO}} \Delta G_{\text{MgO}}^* + X_{\text{SiO}_2} \Delta G_{\text{SiO}_2}^*] \\ &+ \Delta G_{\text{Mix}}^*(\text{CaO-SiO}_2) + \Delta G_{\text{Mix}}^*(\text{Fe}_n\text{O-SiO}_2) \\ &+ \Delta G_{\text{Mix}}^*(\text{MgO-SiO}_2) + \text{GCAFESI} + \text{GCAMGSI} + \text{GFEMGSI} \end{aligned} \quad (7)$$

$$\begin{aligned} \Delta G^*(\text{Fe}_n\text{O-MgO-MnO-SiO}_2) &= [X_{\text{Fe}_n\text{O}} \Delta G_{\text{Fe}_n\text{O}}^* + X_{\text{MgO}} \Delta G_{\text{MgO}}^* + X_{\text{MnO}} \Delta G_{\text{MnO}}^* \\ &+ X_{\text{SiO}_2} \Delta G_{\text{SiO}_2}^*] + \Delta G_{\text{Mix}}^*(\text{Fe}_n\text{O-SiO}_2) + \Delta G_{\text{Mix}}^*(\text{MgO-SiO}_2) \\ &+ \Delta G_{\text{Mix}}^*(\text{MnO-SiO}_2) + \text{GFEMGSI} + \text{GFEMNSI} \end{aligned} \quad (8)$$

$$\begin{aligned} \Delta G^*(\text{CaO-MgO-MnO-SiO}_2) &= [X_{\text{CaO}} \Delta G_{\text{CaO}}^* + X_{\text{MgO}} \Delta G_{\text{MgO}}^* + X_{\text{MnO}} \Delta G_{\text{MnO}}^* + X_{\text{SiO}_2} \Delta G_{\text{SiO}_2}^*] \\ &+ \Delta G_{\text{Mix}}^*(\text{CaO-SiO}_2) + \Delta G_{\text{Mix}}^*(\text{MgO-SiO}_2) + \Delta G_{\text{Mix}}^*(\text{MnO-SiO}_2) \\ &+ \text{GCAMGSI} + \text{GCAMNSI} \end{aligned} \quad (9)$$

$$\begin{aligned} \Delta G^*(\text{CaO-Fe}_n\text{O-MgO-MnO-SiO}_2) &= [X_{\text{CaO}} \Delta G_{\text{CaO}}^* + X_{\text{Fe}_n\text{O}} \Delta G_{\text{Fe}_n\text{O}}^* + X_{\text{MgO}} \Delta G_{\text{MgO}}^* \\ &+ X_{\text{MnO}} \Delta G_{\text{MnO}}^* + X_{\text{SiO}_2} \Delta G_{\text{SiO}_2}^*] \\ &+ \Delta G_{\text{Mix}}^*(\text{CaO-SiO}_2) + \Delta G_{\text{Mix}}^*(\text{Fe}_n\text{O-SiO}_2) + \Delta G_{\text{Mix}}^*(\text{MnO-SiO}_2) \\ &+ \Delta G_{\text{Mix}}^*(\text{MgO-SiO}_2) + \text{GCAFESI} + \text{GCAMGSI} + \text{GCAMNSI} \\ &+ \text{GFEMGSI} + \text{GFEMNSI} \end{aligned} \quad (10)$$

The model parameters,  $\Delta G_{\text{CaO}}^*$ ,  $\Delta G_{\text{FeO}}^*$ ,  $\Delta G_{\text{MgO}}^*$ ,  $\Delta G_{\text{MnO}}^*$ ,  $\Delta G_{\text{SiO}_2}^*$ ,  $\Delta G_{\text{Mix}}^*(\text{CaO-SiO}_2)$ ,  $\Delta G_{\text{Mix}}^*(\text{Fe}_n\text{O-SiO}_2)$ ,  $\Delta G_{\text{Mix}}^*(\text{MgO-SiO}_2)$ ,  $\Delta G_{\text{Mix}}^*(\text{MnO-SiO}_2)$ , GCAFESI, GCAMGSI, FCAMNSI, GFEMGSI, and GFEMNSI in these equations can be found in Table VII. In order to examine the reliability of the model calculations, the calculated viscosity values are

Table VII. Optimized Model Parameters

Component <i>i</i>	Density (g · cm <sup>-3</sup> )	Molar weight (g · mol <sup>-1</sup> )	$\Delta G^*$ (J · mol <sup>-1</sup> )
CaO	3.3	56.079	$1.85327311 \times 10^5$
Fe <sub>n</sub> O	4.7	71.846	$1.33749591 \times 10^5 - 18.0328243T$
MgO	3.58	40.311	$1.86541828 \times 10^5$
MnO	5.43	70.937	$1.32713886 \times 10^5$
SiO <sub>2</sub>	2.3	60.085	$5.33067968 \times 10^5 - 53.2975311T$
$\Delta G_{\text{Mix}}^*$ (J · mol <sup>-1</sup> )			
Binary interaction			
CaO-SiO <sub>2</sub>	$\Delta G_{\text{Mix}}^*(\text{CaO-SiO}_2) = y_{\text{Ca}}^{2+} y_{\text{Si}}^{4+} [ -8.56218889 \times 10^5 + 103.733092T + 2.64594343 \times 10^5 (y_{\text{Ca}}^{2+} - y_{\text{Si}}^{4+}) ]$		
Fe <sub>n</sub> O-SiO <sub>2</sub>	$\Delta G_{\text{Mix}}^*(\text{Fe}_n\text{O-SiO}_2) = y_{\text{Fe}}^{2+} y_{\text{Si}}^{4+} [ -9.70281422 \times 10^5 + 242.480930T + 1.90586769 \times 10^5 (y_{\text{Fe}}^{2+} - y_{\text{Si}}^{4+}) ]$		
MgO-SiO <sub>2</sub>	$\Delta G_{\text{Mix}}^*(\text{MgO-SiO}_2) = y_{\text{Mg}}^{2+} y_{\text{Si}}^{4+} [ -8.18430330 \times 10^5 + 91.3638027T + 1.35009560 \times 10^5 (y_{\text{Mg}}^{2+} - y_{\text{Si}}^{4+}) ]$		
MnO-SiO <sub>2</sub>	$\Delta G_{\text{Mix}}^*(\text{MnO-SiO}_2) = y_{\text{Mn}}^{2+} y_{\text{Si}}^{4+} [ -7.30955356 \times 10^5 + 85.8415806T - 7.47554681 \times 10^4 (y_{\text{Mn}}^{2+} - y_{\text{Si}}^{4+}) ]$		
Ternary interaction			
CaO-Fe <sub>n</sub> O-SiO <sub>2</sub>	$\Delta G_{\text{Mix}}^*(\text{CaO-Fe}_n\text{O-SiO}_2) = \Delta G_{\text{Mix}}^*(\text{CaO-SiO}_2) + \Delta G_{\text{Mix}}^*(\text{Fe}_n\text{O-SiO}_2) + \text{GCAFESI}$ GCAFESI = $y_{\text{Ca}}^{2+} y_{\text{Fe}}^{2+} y_{\text{Si}}^{4+} (1.14932406 \times 10^6 - 139.466890T - 1.05268958 \times 10^6 y_{\text{Ca}}^{2+} - 1.18703224 \times 10^6 y_{\text{Fe}}^{2+})$		
CaO-MgO-SiO <sub>2</sub>	$\Delta G_{\text{Mix}}^*(\text{CaO-MgO-SiO}_2) = \Delta G_{\text{Mix}}^*(\text{CaO-SiO}_2) + \Delta G_{\text{Mix}}^*(\text{MgO-SiO}_2) + \text{GCAMGSI}$ GCAMGSI = $y_{\text{Ca}}^{2+} y_{\text{Mg}}^{2+} y_{\text{Si}}^{4+} (1.07014539 \times 10^6 - 324.501809T)$		
CaO-MnO-SiO <sub>2</sub>	$\Delta G_{\text{Mix}}^*(\text{CaO-MnO-SiO}_2) = \Delta G_{\text{Mix}}^*(\text{CaO-SiO}_2) + \Delta G_{\text{Mix}}^*(\text{MnO-SiO}_2) + \text{GCAMNSI}$ GCAMNSI = $y_{\text{Ca}}^{2+} y_{\text{Mn}}^{2+} y_{\text{Si}}^{4+} (-6.75779022 \times 10^5 + 504.161763T)$		
Fe <sub>n</sub> O-MgO-SiO <sub>2</sub>	$\Delta G_{\text{Mix}}^*(\text{Fe}_n\text{O-MgO-SiO}_2) = \Delta G_{\text{Mix}}^*(\text{FeO-SiO}_2) + \Delta G_{\text{Mix}}^*(\text{MgO-SiO}_2) + \text{GFEMGSI}$ GFEMGSI = $y_{\text{Fe}}^{2+} y_{\text{Mg}}^{2+} y_{\text{Si}}^{4+} (7.83484279 \times 10^5 - 271.089792T)$		
Fe <sub>n</sub> O-MnO-SiO <sub>2</sub>	$\Delta G_{\text{Mix}}^*(\text{Fe}_n\text{O-MnO-SiO}_2) = \Delta G_{\text{Mix}}^*(\text{Fe}_n\text{O-SiO}_2) + \Delta G_{\text{Mix}}^*(\text{MnO-SiO}_2) + \text{GFEMNSI}$ GFEMNSI = $y_{\text{Fe}}^{2+} y_{\text{Mn}}^{2+} y_{\text{Si}}^{4+} (1.66129998 \times 10^6 - 891.715429T)$		

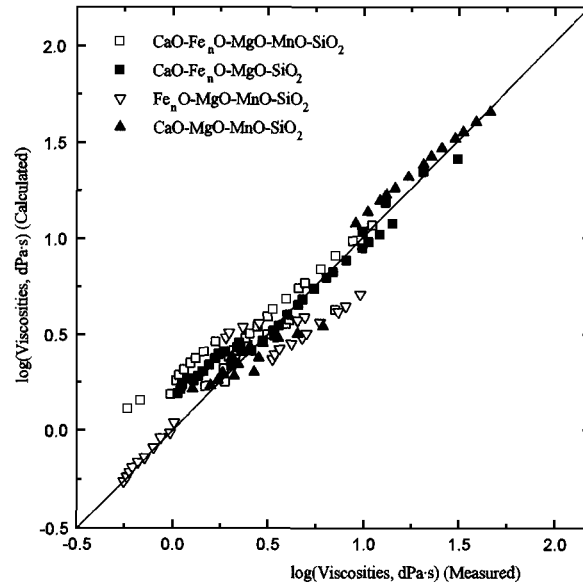


Fig. 2. Comparison of calculated results with measured viscosity values in the three quarternary and one quinary systems.

compared with the experimental data in Fig. 2. It should be emphasized that in all the calculations, the viscosities were calculated based only on the model parameters of low-order interactions. The experimental data for the higher-order systems, *viz.*, quarternary and quinary systems were not used. It is shown in Fig. 2 that the results of the model calculations are in good agreement with the experimental data in the case of all four systems, thereby confirming the reliability of the viscosity model in predicting the viscosities for higher-order systems.

Equations (7) to (10) provide useful tools for predicting the viscosities of the  $\text{CaO-Fe}_n\text{O-MgO-SiO}_2$ ,  $\text{Fe}_n\text{O-MgO-MnO-SiO}_2$ ,  $\text{CaO-MgO-MnO-SiO}_2$ , and  $\text{CaO-Fe}_n\text{O-MgO-MnO-SiO}_2$  melts at any given temperature. Figure 3 presents the viscosities in the  $\text{CaO-Fe}_n\text{O-MgO-SiO}_2$  and  $\text{Fe}_n\text{O-MgO-MnO-SiO}_2$  systems at different temperatures with constant mole fractions of MgO and  $\text{SiO}_2$ , *viz.*,  $X_{\text{MgO}} = 0.08$  and  $X_{\text{SiO}_2} = 0.20$ . It is seen that the viscosities in these two systems decrease when the temperature is increased. While the viscosity in the  $\text{Fe}_n\text{O-MgO-MnO-SiO}_2$  system does not show a significant dependence on the FeO content, the viscosity in the  $\text{CaO-Fe}_n\text{O-MgO-SiO}_2$  system decreases with increasing mole fraction of FeO. It is well known that the addition of metal oxides breaks down the silicate groups and thereby decreases the viscosity of the

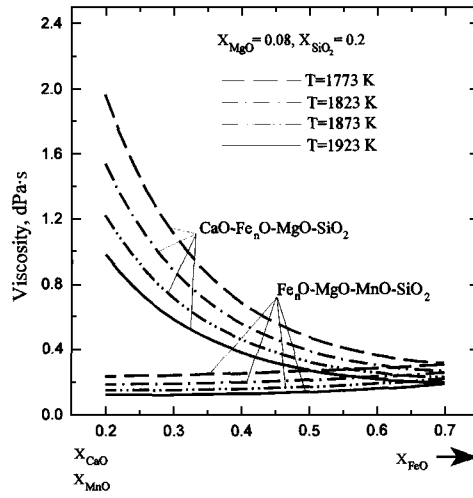


Fig. 3. Viscosities as functions of the mole fraction of  $Fe_nO$  in the  $CaO-Fe_nO-MgO-SiO_2$  and  $Fe_nO-MgO-MnO-SiO_2$  systems at different temperatures, with  $X_{MgO} = 0.08$  and  $X_{SiO_2} = 0.20$ .

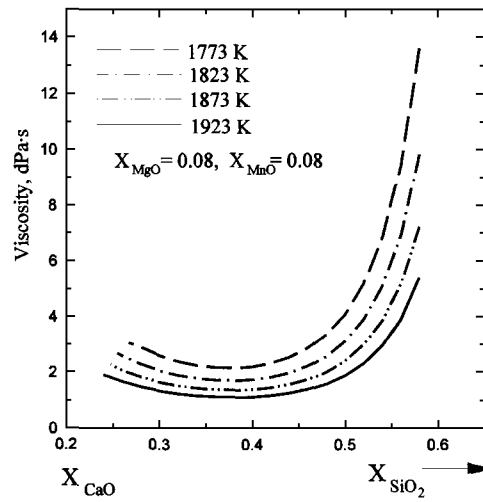


Fig. 4. Viscosities as functions of the mole fraction of  $SiO_2$  in the  $CaO-MgO-MnO-SiO_2$  system at different temperatures, with  $X_{MgO} = 0.08$  and  $X_{MnO} = 0.08$ .

melt. The melt will consist primarily of small  $\text{SiO}_4^{4-}$  groups when the mole fraction of  $\text{SiO}_2$  is only 0.2. Hence, the role of the cation size and the electropositive character seem to be important.

In Fig. 4, the viscosities at different temperatures in the  $\text{CaO-MgO-MnO-SiO}_2$  system at  $X_{\text{MgO}}=0.08$  and  $X_{\text{MnO}}=0.08$  are plotted as functions of the  $\text{SiO}_2$  content. The viscosity decreases considerably when the mole fraction of  $\text{SiO}_2$  is decreased from 0.58 to 0.45. Beyond this region, the fast decrease in viscosity with the increase of the basic oxide content is not observed. The viscosity even shows a slight increase when the slag composition is approaching the saturation of  $\text{CaO}$ . The melts containing 0.58 mol fraction of  $\text{SiO}_2$  are very close to  $\text{SiO}_2$  saturation. It is reasonable to expect that the slag still retains the network structure partially, which makes the melt viscous. The additions of the metal oxides will break down the silicate network and decrease the viscosity of the melt. When the total mole fraction of cations reaches 0.55, the melt will consist primarily of small  $\text{SiO}_4^{4-}$  groups. Therefore, the further addition of metal oxides does not affect the viscosity to any great extent.

Figure 5 presents the calculated isoviscosity lines for the  $\text{CaO-Fe}_n\text{O-MgO-MnO-SiO}_2$  system at 1873 K and  $X_{\text{MgO}}=0.05$  and  $X_{\text{MnO}}=0.05$ . While in the  $\text{SiO}_2$ -rich region, the increase in the  $\text{SiO}_2$  content increases the viscosity dramatically, the effect of the  $\text{CaO}$  content on the viscosity

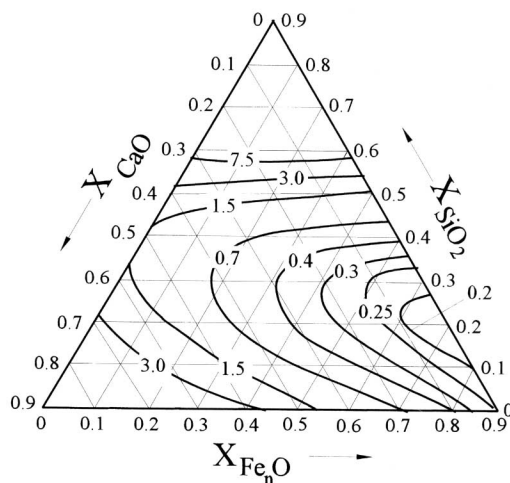


Fig. 5. Isoviscosity contours in the  $\text{CaO-Fe}_n\text{O-MgO-MnO-SiO}_2$  system at 1873 K, with  $X_{\text{MgO}}=0.05$  and  $X_{\text{MnO}}=0.05$ .

becomes important in the low-SiO<sub>2</sub>-containing melts. This observation is in accordance with the results shown in Fig. 4.

## REFERENCES

1. Du Sichen, J. Bygden, and S. Seetharaman, *Met. Mat. Trans. B* **25**:1 (1994).
2. F.-Z. Ji, Du Sichen, and S. Seetharaman, *TRATA MEL* **176**:April (1997), Theoretical Metallurgical Metallurgy, Royal Institute of Technology, Stockholm, Sweden.
3. F.-Z. Ji, Du Sichen, and S. Seetharaman, *Met. Mat. Trans. B* **28**:827 (1997).
4. F.-Z. Ji, Du Sichen, and S. Seetharaman, *Ironmaking and Steelmaking* (in press, 1998).
5. I. Tanabe, K. Oku, and T. Honda, *J. Electrochem. Soc. Japan* **28**:E288 (1960).
6. E. M. Levin, C. R. Robbins, and H. F. McMurbie, *Phase Diag. ceram. Am. Ceram. Soc.* **1**:38 (1964).
7. K. C. Mills and A. A. Shirali, *SRM for High Temperature Viscosities Measurements—Results for Phase 3 of the Interlaboratory Comparison Programme*, NPL report (National Physical Laboratory, Teddington, Middlesex, UK, 1993).